WILEY | Hindawi

Research Article

Fractional-Derivative Approximation of Relaxation in Complex Systems

Kin M. Li,[1] Mihir Sen,[2] and Arturo Pacheco-Vega [1]

[1]*Department of Mechanical Engineering, California State University-Los Angeles, Los Angeles, CA 90032, USA*
[2]*Department of Aerospace and Mechanical Engineering, University of Notre Dame, Notre Dame, IN 46556, USA*

Correspondence should be addressed to Arturo Pacheco-Vega; apacheco@calstatela.edu

In this paper, we present a system identification (SI) procedure that enables building linear time-dependent fractional-order differential equation (FDE) models able to accurately describe time-dependent behavior of complex systems. The parameters in the models are the order of the equation, the coefficients in it, and, when necessary, the initial conditions. The Caputo definition of the fractional derivative, and the Mittag-Leffler function, is used to obtain the corresponding solutions. Since the set of parameters for the model and its initial conditions are nonunique, and there are small but significant differences in the predictions from the possible models thus obtained, the SI operation is carried out via global regression of an error-cost function by a simulated annealing optimization algorithm. The SI approach is assessed by considering previously published experimental data from a shell-and-tube heat exchanger and a recently constructed multiroom building test bed. The results show that the proposed model is reliable within the interpolation domain but cannot be used with confidence for predictions outside this region. However, the proposed system identification methodology is robust and can be used to derive accurate and compact models from experimental data. In addition, given a functional form of a fractional-order differential equation model, as new data become available, the SI technique can be used to expand the region of reliability of the resulting model.

1. Introduction

Complex systems are common in mechanical engineering applications, for example, automobiles, washing machines, and thermal power plants. As illustrated schematically in Figure 1, each of these systems is composed of many interconnected subsystems. In principle each subsystem can be studied in isolation and its input and output connected to others. However, for purposes of control we may think of the overall system as being of the single-input single-output (SISO) type, i.e., the interconnections between subsystems are all internal, and there is only a single input $u(t)$ and a single output $y(t)$ of the overall system, where t is time. The control of such systems may either be model based or not [1]. Control procedures that are not based on a mathematical model include techniques such as PID [2], fuzzy logic [3], or other procedures that work on the error signal. For model based control, on the other hand, one should have an approximate mathematical model of the time-dependent

behavior of the system to be able to predict what is going to happen and then control it (approximate because otherwise there would be no need for control). For simplicity we will only consider linear systems. There are two types of inputs that are of interest in complex SISO systems: one is relaxation and the other is periodic. In the former, which is what we will be concerned with here, a step input is applied to the system and the output goes in some dynamic fashion from one constant value to another.

One approach to modeling is from the ground up, i.e., to use first principles to model each component and their interactions to create a so-called white box model. If we think of each subsystem as being governed by a single ordinary differential equation (ODE), then the overall system is governed by a large set of coupled ODEs. If, however, there is a governing partial differential equation (PDE), then that may be considered to be equivalent to an infinite set of ODEs. Modeling is possible only when there is physical and mathematical understanding of the behavior of each
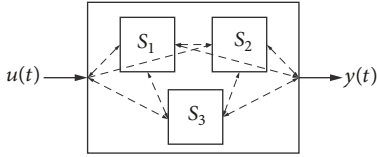
FIGURE 1: Schematic representation of a complex system with subsystems S_1, S_2, and S_3. Dashed lines are interactions. Input and output of the overall system are $u(t)$ and $y(t)$, respectively.

subsystem. In any case, for control of the overall system one ends up working with a large set of ODEs that must be solved in real time. This may be computationally undesirable for control purposes.

In many cases it is advantageous to use existing or continually acquired experimental data to make predictions [4]. This is a black-box approach and its main advantage is that the input-output response of the overall system can be directly obtained, but a disadvantage is that there is no physical understanding of the dynamic behavior compared to the ground-up approach. For example, one can have a procedure based on artificial neural networks which can either be trained beforehand or continuously trained [5]. Alternatively one can fit an analytical model to the data, and this is *system identification* (SI). For control purposes the data-based model should be good enough to approximate reality but also be solvable in real time without intensive computation. The SI process leads to a mathematical model that can make predictions that differ little from reality in the region of interest and is compact enough to be easily solved and used for control purposes. The most common SI procedure is to propose a mathematical model of the relaxation dynamics of the system, usually in the form of differential equations, with certain free constants that are adjusted to best fit measurements. In this manifestation SI is really determination of parameters in the proposed model.

Two new aspects will be explored here in relation to SI.

(a) Fractional-Order Model. Usually the proposed mathematical models involve integer-order derivatives, but this lacks the generality provided by derivatives of fractional order [6–8]. In addition, the required mathematical description of the system is directly linked to its complexity, and when the latter increases so does the former. Though any system representation can be achieved using integer-order conservation equations, their solution, in the context of system control, requires extremely large CPU times, and it becomes necessary to develop accurate and compact models that can be used to determine the corresponding behavior in a timely and reliable manner. Since it has been recently demonstrated that fractional-based models are able to describe systems that are complex [9], and a physical understanding of the subsystem processes is not of concern for control of the overall system, the use of suitably defined fractional derivatives is appropriate [10, 11]. There are many different definitions of fractional derivatives available, though there are some common features between them [12]. Initial conditions for

time-dependent systems is an important issue for fractional-order systems: unlike integer-order derivatives where the number of initial conditions corresponds to the order of the differential equation, many of the definitions of fractional derivatives make the equation infinite dimensional so that an infinite number of initial conditions are needed. Here we use the Caputo definition of the fractional derivative since it enables the prescription and application of initial conditions of integer order typically encountered in physical systems, and analytical solutions are often possible.

(b) Error Minimization by Global Regression. The mathematical model with the best approximation to experimental data is obtained through a process of error minimization. On the one hand this can be done through an algorithm that searches locally in the neighborhood of an initial guess, a procedure that is effective if there is a single minimum. On the other hand there are procedures that search globally within the permitted range of parameters for one or more minima. One of these techniques is that of genetic algorithms [4] and another is simulated annealing, which is what we will use here [13, 14].

In the present investigation, we propose a methodology of analysis to derive accurate models – based on fractional-order differential equations – that approximate relaxation processes of complex systems. To this end, the paper presents first a brief description of the background information about fractional calculus. Next, the system identification technique, based on global regression of an error-cost function, is introduced in detail. Application to previously published experimental data derived from (1) a heat exchanger and (2) a recently constructed building test facility is later carried out with special emphasis on the accuracy of the model within the region of interest. A vital conclusion is the nonuniqueness in the resulting parameter set that defines both the fractional-order model and the corresponding initial conditions. Although the proposed model is accurate within the interpolation region, it is unreliable outside it.

2. Background on Fractional Calculus

Fractional (noninteger) calculus, which can be thought of as a generalization of the well-known integer calculus, has a long history dating back to Leibniz [9]. Nevertheless, it is not as celebrated by the scientific community as its integer counterpart, mainly due to insufficient enthusiasm about its potential usefulness in applications. Although significant progress in its theoretical basis has been achieved, primarily due to contributions from 18th- and 19th-century mathematicians (e.g., Laplace, Fourier, Abel, and Liouville), it is only in the last two decades that the subject has significantly broadened its applications in physics and engineering. This is reflected by the increased number of publications (i.e., books [9, 15–17], review monograms [10], and scientific articles) devoted to the topic in a variety of fields, like anomalous diffusion [18], semi-infinite tree networks of mechanical, electrical, and hydrodynamic equipment [19, 20], and viscoelastic systems [21], among others. In the context of modeling and control of thermal devices and phenomena, studies, such as those

of Aoki et al. [22], Pineda et al. [23], Gabano and Poinot [24], and Caponetto et al. [25], demonstrate that fractional derivatives provide good approximations for describing the dynamic behavior of heat transfer processes.

In principle, the field of fractional calculus entails the generalization of the concept of a derivative beyond that of the common integer order. It is concerned with the meaning of the "in-between" derivatives. For instance, the 5/4-derivative of a function $f(t)$,

$$f^{(5/4)}(t) = \frac{d^{5/4} f}{dt^{5/4}} \tag{1}$$

can be thought of as a derivative in-between the first and second derivatives. Though it seems straightforward to think of a derivative whose order is between two consecutive integers, the definition of a fractional derivative is not unique and various definitions are possible as long as it satisfies a required set of mathematical rules [12]. Two of the most common definitions are those of Riemann-Liouville [16] and Caputo [26], the latter being the type of derivative used in the present study.

Let us start with the Cauchy formula for repeated integrals of integer order m, for the function $f(t)$, which is defined as

$$J^m f(t) = \frac{1}{(m-1)!} \int_0^t (t-z)^{m-1} f(z)\, dz; \quad m \in \mathbb{Z}, \tag{2}$$

where J^m is the integral operator. By defining the Gamma function as

$$\Gamma(\xi) = \int_0^\infty e^{-t'} t'^{\xi-1} dt', \tag{3}$$

the term $(m-1)!$ in (2) can be replaced with $\Gamma(\alpha)$, to obtain

$$J^\alpha f(t) = \frac{1}{\Gamma(\alpha)} \int_0^t (t-z)^{\alpha-1} f(z)\, dz, \tag{4}$$

where $\alpha > 0$ is an arbitrary positive real number and z is a dummy variable of integration. Note that $J^\alpha f(t) = D^{-\alpha} f(t)$; thus, for a value of α such that $m - 1 < \alpha \le m$

$$D_{RL}^\alpha f(t) = D^m J^{m-\alpha} f(t), \tag{5}$$

which establishes the Riemann-Liouville fractional derivative of order α, as

$$D_{RL}^\alpha f(t) = \frac{d^m}{dt^m} \left[\frac{1}{\Gamma(m-\alpha)} \int_0^t \frac{f(z)}{(t-z)^{\alpha+1-m}} dz \right]. \tag{6}$$

The Caputo definition of the fractional derivative of order α, on the other hand, is defined as [26]

$$D_C^\alpha f(t) = J^{m-\alpha} D^m f(t), \tag{7}$$

so that $D_C^\alpha f(t)$ is explicitly given as

$$D_C^\alpha f(t) = \frac{1}{\Gamma(m-\alpha)} \int_0^t \frac{f^{(m)}(z)\, dz}{(t-z)^{\alpha+1-m}}. \tag{8}$$

In (6) and (8), the subscripts RL and C, respectively, denote Riemann-Liouville and Caputo fractional derivatives.

Regardless of the definition used, the Laplace transform is a powerful technique to solve equations involving fractional derivatives. For instance, the Riemann-Liouville definition in the Laplace domain is

$$\mathscr{L}\left(D_{RL}^\alpha f(t)\right) = s^\alpha F(s) - \sum_{k=0}^{m-1} s^k D^{\alpha-k-1} f(0); \tag{9}$$

$$m - 1 < \alpha \le m,$$

where it can be seen that the transformation requires the following initial conditions: $D^{\alpha-k-1} f(0)$ for all $0 \le k \le m - 1$. It is important to note that, since α does not need to be an integer number, the terms $D^{\alpha-k-1} f(0)$ are all of fractional order. This poses a problem for applications in physical systems, where the initial conditions are typically given in terms of integer orders. On the other hand, the Laplace transform for the Caputo definition is

$$\mathscr{L}\left(D_C^\alpha f(t)\right) = s^\alpha F(s) - \sum_{k=0}^{m-1} s^{\alpha-k-1} D^k f(0); \tag{10}$$

$$m - 1 < \alpha \le m,$$

where now the initial conditions necessary to evaluate (10) are prescribed as integer order, $D^k f(0)$, rather than fractional-order derivatives. Therefore, in the subsequent sections of the paper, we use the Caputo definition of a fractional-order derivative.

3. System Identification

The first step in the SI process is to propose the model and then to determine the parameters therein that will approximate – as closely as possible – its output to the target data. For our purposes, the proposed model is the linear fractional differential equation, given as

$$c_1 \frac{d^q y(t)}{dt^q} + c_2 y(t) = u(t), \tag{11}$$

where c_1 and c_2 are constants, q is the order (noninteger, $m - 1 < q \le m$, with $m \in \mathbb{Z}$) of the equation, $u(t)$ is its input, $y(t)$ is the corresponding output, and t is a time-like independent variable. Since the interest is on the conditions of operation that would take the system from one state to another, i.e., relaxation processes, taking $u(t)$ to be the Heaviside function, the Laplace transform of (11) is

$$Y(s) = \frac{\sum_{k=0}^m s^{q-k-1} y^{(k)}(0)}{s^q + c_2/c_1} + \frac{1}{c_1} \frac{s^{-1}}{s^q + c_2/c_1}, \tag{12}$$

which can then be solved if the initial conditions for $y(t)$, and its corresponding derivatives, are provided. The inverse Laplace transform of the above equation leads to the following analytical form for $y(t)$

$$y(t) = \sum_{k=1}^m P_k t^{k-1} E_{q,k}\left(-\frac{c_2}{c_1} t^q\right) + \frac{1}{c_1} t^q E_{q,q+1}\left(-\frac{c_2}{c_1} t^q\right), \tag{13}$$

where E is the typical Mittag-Leffler function [17]. Note that the output from (13) is completely defined if the constants P_k are known. This implies that one must provide m derivatives at $t = 0$ ($P_k = y^{(k-1)}(0)$, $k = 1, 2, \ldots, m$); i.e., for $0 \leq q \leq 1$, $y(0)$, and for $1 < q \leq 2$, $y(0)$, and $y'(0)$ are necessary to determine the solution.

To find the unknowns q, c_1, c_2, P_k, for $k = 1, 2, \ldots, m$, in (11) and (13), from known data (e.g., N values y_i, $i = 1, \ldots, N$), a least-squares method is used to minimize the difference between the sample- and predicted-values of $y(t)$. This is equivalent to minimizing an Euclidean norm, i.e., the variance of the error, given by

$$S_y = \frac{1}{N} \sum_{i=1}^{N} \left(y_i^p - y_i^e \right)^2, \tag{14}$$

where N is the number of data points, usually from experimental measurements; $y_i^p(t)$, for $i = 1, \ldots, N$, are values predicted by the model and $y_i^e(t)$, for $i = 1, \ldots, N$, refer to the experiments. It is to be noted that $S_y(\mathbf{C})$, with $\mathbf{C} = (q, c_1, c_2, P_k : k = 1, \ldots, m)$ being the vector of unknown parameters, is a smooth manifold in a $(k + 3)$-dimensional space. The goal is now to search for the values of the parameter set $\mathbf{C}$, such that $S_y(\mathbf{C})$ is a minimum. This process can be carried out either using local – such as gradient-based – methods or global optimization techniques like evolutionary or deterministic algorithms, each with advantages and drawbacks [27–31]. However, as we will show in a later section, under certain cases (14) has multiple local minima, stemming from its nonlinear nature with respect to the arguments, thus leading us to seek the global minimum which will provide the optimal values of the parameter set $\mathbf{C}$ required in the model (11), and the corresponding initial conditions. This optimization procedure is carried out here by the *simulated annealing* (SA) technique.

Description. The SA technique is inspired by the molecular calculation of the cooling of a physical system in which random agitation is used to avoid entrapment in local extrema [29]. A starting point in the space of unknowns, $\mathbf{C}_0$, is randomly selected, and a cycle of random moves along each coordinate direction is then performed. The new point $\mathbf{C}$ is accepted if it gives a better value of S_y. If it is worse, it is accepted only with a certain probability, $\exp(-\Delta S_y / T^*)$, where ΔS_y is the change in value of S_y and T^* is a dynamic parameter that is analogous to the temperature of a system being cooled [32]. The process is repeated with decreasing T^*, and step size $\Delta \mathbf{C}$ until convergence within a certain tolerance is reached. The procedure described above [33] has been successfully implemented and used in the context of heat transfer correlations by Pacheco-Vega et al. [34], and it is the one followed here.

It is to be noted that other global optimization algorithms can also be used in the search for the set of parameters $\mathbf{C}$. These include the popular genetic algorithm (GA) [28] and the interval method (IM) [35], among several alternatives, which have been successfully used in a variety of applications. Though each technique has advantages over the others (particularly in terms of CPU time necessary to find

a solution), the GA will only find the region – with a high degree of certainty – where the global optimum is located. From this perspective, only IMs mathematically guarantee that the global optimum has been found, while the SA is only probabilistically – but not deterministically – guaranteed to find such an optimum solution.

SI using the fractional model in (11), herein referred to as FOSI, is applied to experimental data from two complex thermal systems: (1) shell-and-tube heat exchanger data analyzed by Mayes [36] and (2) a multiroom building test facility. Preliminary analysis on the applicability of the FOSI methodology to a set of analytical problems and to heat exchanger data has been recently reported in Li et al. [37]. In what follows, the search domain for q, in (11), is restricted to $q \in [0, m]$ with $m = 2$.

4. Shell-and-Tube Heat Exchanger Data

4.1. Description. Details about the experimental setup in the thermal systems laboratory at the University of Notre Dame, and the corresponding data obtained with it, have been reported in Mayes [36]; here we provide only a brief description of the problem at hand. The heat exchanger, a schematic of which is shown in Figure 2, corresponds to the common shell-and-tube configuration. The figure illustrates flow directions of the cold and hot fluids, $\dot{m}_c$ and $\dot{m}_h$, respectively, along with their corresponding terminal inlet, T_c^{in} and T_h^{in}, and outlet, T_c^{out} and T_h^{out}, bulk temperatures. The reported tests [36] were carried out under time-dependent conditions until thermal equilibrium in the device was achieved. Subsequently, while maintaining constant values of T_c^{in}, T_h^{in}, and $\dot{m}_h$, a step change in $\dot{m}_c$, i.e., $\Delta \dot{m}_c$, was applied. A data acquisition system (DAQ) and a personal computer (PC) were used to record and store the time-dependent values of the inlet and outlet temperatures of the two fluids.

For purposes of analysis, we take the approach of [36] and work with normalized variables. The dimensionless outlet temperature of the hot fluid θ and time variable τ are defined as

$$\theta(t) = \frac{T_h^{out}(t) - T_h^{out}(0)}{T_h^{out}(\infty) - T_h^{out}(0)}; \quad \tau = \frac{t}{\tau_r}, \tag{15}$$

where $T_h^{out}(0)$ and $T_h^{out}(\infty)$ are, respectively, the values of hot-fluid outlet temperatures at the initial and steady states; τ_r is the rise time, defined as the time required for $T_h^{out}(t)$ to reach 85% of $T_h^{out}(\infty)$. Thus, $\theta(\tau) \in [0, 1]$, with $\tau \in [0, \infty)$. The experiments showing the temporal evolution of $\theta(\tau)$ are illustrated graphically in Figure 3(a), where it is clear that some type of relaxation process from one state (with θ having a small positive value) to another (where θ is close to 0.8) took place. Since the goal here is to find the parameters in the fractional model of the form given by (11) which fit the experimental data the best, for clarity we define $\theta(\tau) \equiv y(t)$ and $\tau \equiv t$, so that the fractional-order differential equation becomes

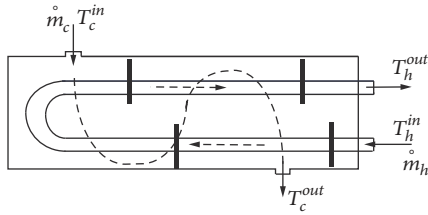$$c_1 \frac{d^q \theta(\tau)}{d\tau^q} + c_2 \theta(\tau) = u(\tau), \tag{16}$$

FIGURE 2: Schematic of a shell-and-tube heat exchanger.

TABLE 1: Model parameters from heat exchanger data.

Model	q	c_1	c_2	$P_2 = \theta'(0)$	$S_\theta \times 10^4$
A	1	-2.4903	0.8055	–	20
B	1.6708	0.3313	1.8067	-0.1093	6.94

where c_1 and c_2 are constants, q is the order in the search domain $q \in [0, m]$, $m = 2$, and $u(t)$ is the input resulting from the step change in the mass flow rate of the cold fluid $\Delta \dot{m}_c$. Once the model has been defined (i.e., Eq. (16)), the FOSI technique is applied to the normalized data.

In this case, the variance of the error is given as

$$S_\theta = \frac{1}{N} \sum_{i=1}^{N} \left(\theta_i^p - \theta_i^e \right)^2, \tag{17}$$

where p and e correspond to predictions and experiments, respectively, and N is the number of data sets. The set of unknown parameters that will be considered in the forthcoming sections will be either $\mathbf{C} = (q, c_1, c_2, P_2 = \theta'(0))$ or $\mathbf{C} = (q, c_1, c_2, P_1 = \theta(0), P_2 = \theta'(0))$. Notice that, when seeking the optimum values in the parameter set, either one $P_2 = \theta'(0)$ or two initial conditions $P_1 = \theta(0)$ and $P_2 = \theta'(0)$ are included; i.e., we have relaxed the restriction regarding the number of unknown parameters and now included either one or two initial conditions in the search. The inclusion of the initial conditions in the parameter search brings the advantage of finding the most appropriate values for them directly from the operating conditions of the system and, therefore, provides a better approximation from the model thus obtained. However, as it will be shown in the next section, this generates multiplicity of solutions of the parameter set, some of which may not be physically feasible.

4.2. Initial Conditions and Nonuniqueness. Initial conditions provide the set of values of the system at the point of departure towards a new set of states. Mathematically, these conditions can be easily set up so that the model can be solved. Experimentally, however, this may not be the case since it is difficult to measure the value of the function (e.g., temperature) at a specific time (e.g., $t = 0$), and even more difficult to establish its rate of change, i.e., the derivative. Sensitivity of the sensors, and even where they are placed, plays a crucial role and increases the uncertainty of the corresponding measurement.

As an example of this situation, let us focus on the experimental measurements of the shell-and-tube heat exchanger described before. The system was analyzed in [36] for dynamic conditions of the outlet temperatures after some thermal equilibrium in the device was achieved. Figure 3(a) shows the experimental data (digitized from [36]) corresponding to the evolution of the dimensionless temperature $\theta(\tau)$. From the figure it can be observed that the general trend in the values of the experimental data near $\tau = 0$

($\tau \in [0, 0.01]$) is to decrease in magnitude before showing a sustained relaxation-type increase (with some variation about the mean values) to about $\theta = 0.8$ at $\tau = 1$. This seems to indicate that, unless sudden changes in temperature occurred in the laboratory, the heat-exchange device might not have actually reached the expected thermal equilibrium, and it raises the question about the actual level of uncertainty that may be present while attempting to accurately establish the initial conditions for complex systems since the values $\theta(0) = 0$ and $\theta'(0) = 0$, in this case, are not feasible.

An example is the case of a sensor measuring temperature that either is not appropriately calibrated or that has a slow response time-constant, then the initial states for the temperature or its rate of change will not be correctly established. In other cases, the system may be so complex that establishing actual initial conditions is virtually impossible. A car comprising a large number of subsystems may have initial states for each of those components that are different than those of the overall system, and deciding which initial state is the most appropriate (and thus, the one that should be used) may be extremely difficult. A similar situation occurs in a fluid, where initial conditions must be specified at all locations. From this perspective, the inclusion of the initial conditions in the unknown parameter set may be advantageous since the optimal values of these states can be directly computed from the data via SI. On the other hand, mathematically, by increasing the number of adjustable parameters it may be possible to obtain a better approximation from the model. This is what we have done within the context of the two thermal systems considered here.

In what follows, we apply the global-regression-based FOSI to the heat exchanger experimental data to obtain the parameters in (16) and – when necessary – the corresponding initial conditions that minimize the variance of the error [Eq. (17)]. The search for the parameters in $\mathbf{C} = (q, c_1, c_2, P_2 = \theta'(0))$ is constrained to the following ranges: $q \in [0, 2]$, $\{c_1, c_2\} \in [-10, 10]$, and $\theta'(0) \in [-10, 10]$. The initial condition is kept as $P_1 = \theta(0) = 0$, as established in [36]. For purposes of comparison, a gradient-based local optimization algorithm (LOA) is also applied to seek the best-possible parameters in $\mathbf{C}$. In applying the LOA technique, the search is constrained only for the order $q \in [0, 2]$, while the domain for all other parameters remains unconstrained.

The results from the two fractional-order models are shown in Figure 3(a) and Table 1. From the figure it can be seen that the model obtained by global regression (model B) provides a much better approximation to the experimental data than that from the local-regression procedure (model A). Although both models are somewhat closer in the middle regions, i.e., $t \in [0.2, 0.8]$, their predictions deviate significantly at the two ends of the relaxation process, with the SA-based model (also referred to as a four-parameter model
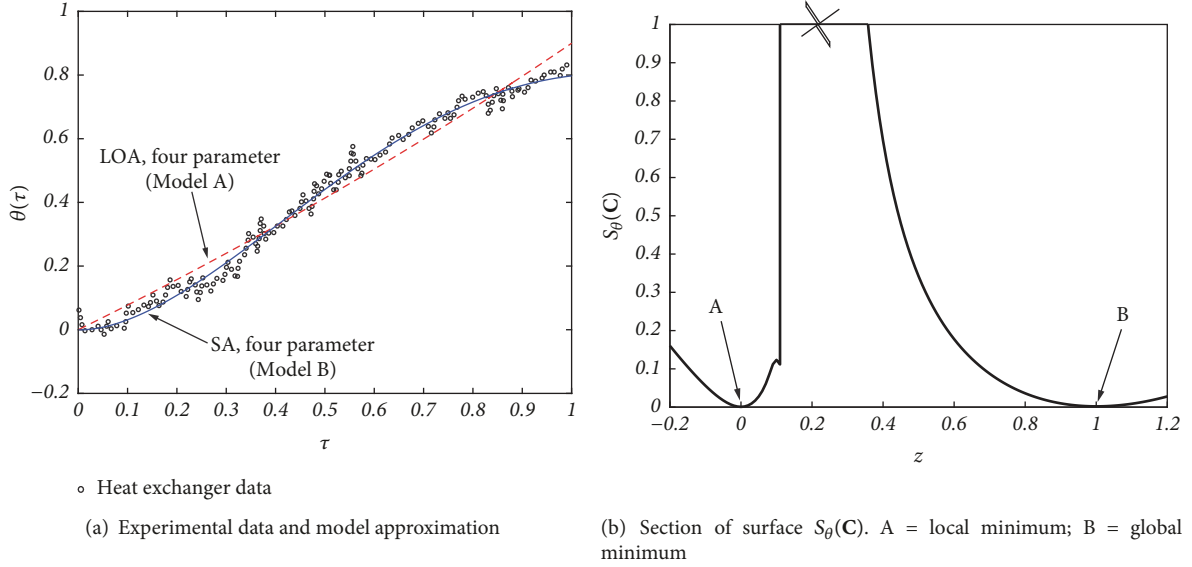
(a) Experimental data and model approximation

(b) Section of surface $S_\theta(\mathbf{C})$. A = local minimum; B = global minimum

FIGURE 3: Multiplicity of solutions in the parameter set $\mathbf{C} = (q, c_1, c_2, P_2 = \theta'(0))$.

TABLE 2: Model parameters from shifted heat exchanger data.

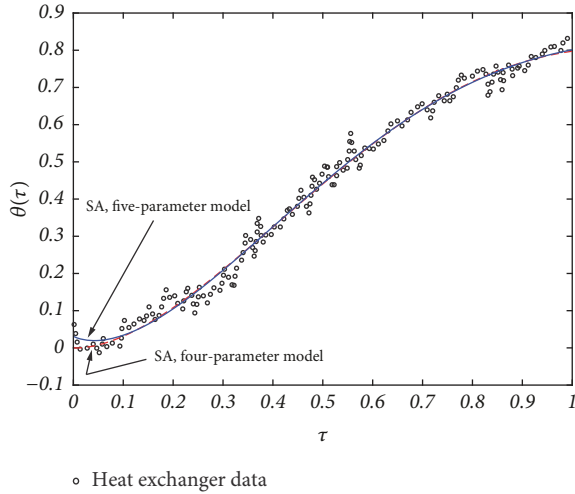|	q	c_1	c_2	$P_1 = \theta(0)$	$P_2 = \theta'(0)$	$S_\theta \times 10^4$
θ_+	1.5061	0.2717	1.3858	0.005	-0.8368	6.6471
θ	1.5061	0.2621	1.3373	0.0313	-0.8366	6.6470
θ_-	1.5061	0.2532	1.2919	0.0576	-0.8364	6.6471

FIGURE 4: Comparison of prediction of $\theta(\tau)$ between four- and five-parameter-set models. (—) five-parameter model, RMS error is 6.647×10^{-4}; (−−) four-parameter model, RMS error is 6.939×10^{-4}.

in Figure 3(a) since the vector $\mathbf{C}$ comprised four parameters) being much closer to the original data. On the other hand, from the table it can be seen that the two fractional models have very different values of the parameters q, c_1, and c_2, and particularly the fact that $\theta'(0) = P_2$ only appears in the fractional-order model obtained via global regression (model B) since its value of q lies between $m = 1$ and $m = 2$. This

outcome is indicative of the nonuniqueness of the resulting fractional differential equation model, along with the initial condition considered in the parameter set $\mathbf{C}$.

Figure 3(b) shows a section of the S_θ hypersurface that passes through the two minima A and B. For clarity, a location coordinate z is defined such that $\mathbf{C} = \mathbf{C}_A(1 - z) + \mathbf{C}_B z$, where $\mathbf{C}_A = (q, c_1, c_2, P_2 = \theta'(0))_A$ and $\mathbf{C}_B = (q, c_1, c_2, P_2 = \theta'(0))_B$, corresponding to the two minima. The value of the cost function S_θ from the LOA-based model (model A) is 3 times higher than that of the SA model (model B in Table 1). The above result leads us to ask which model is better, and a possible answer may be the model equation that provides the minimum error, i.e., the global minimum. This is accomplished in the present study through the implementation of SA in the SI methodology.

By using the heat exchanger data described before, and relaxing the restriction on the number of parameters in $\mathbf{C}$ to now include the additional initial condition $\theta(0) = P_1$, $\mathbf{C} = (q, c_1, c_2, P_1 = \theta(0), P_2 = \theta'(0))$, i.e., a five-parameter fractional-order model, then it is clear as illustrated in Figure 4 that not only the overall solution but also the value of $\theta(0)$ is much closer to the target data than that of the four-parameter model. It is to be noted that, although not shown explicitly, there is also a multiplicity of solutions in $S_\theta(\mathbf{C})$, the global optimum being found by the SA algorithm. The multiplicity in the parameter set seems to be due to the fact that the initial condition(s) is(are) included in the search rather than the model itself. Finally, Table 2 shows, quantitatively, the improved accuracy of the five-parameter

(a) Predictions in interpolated region
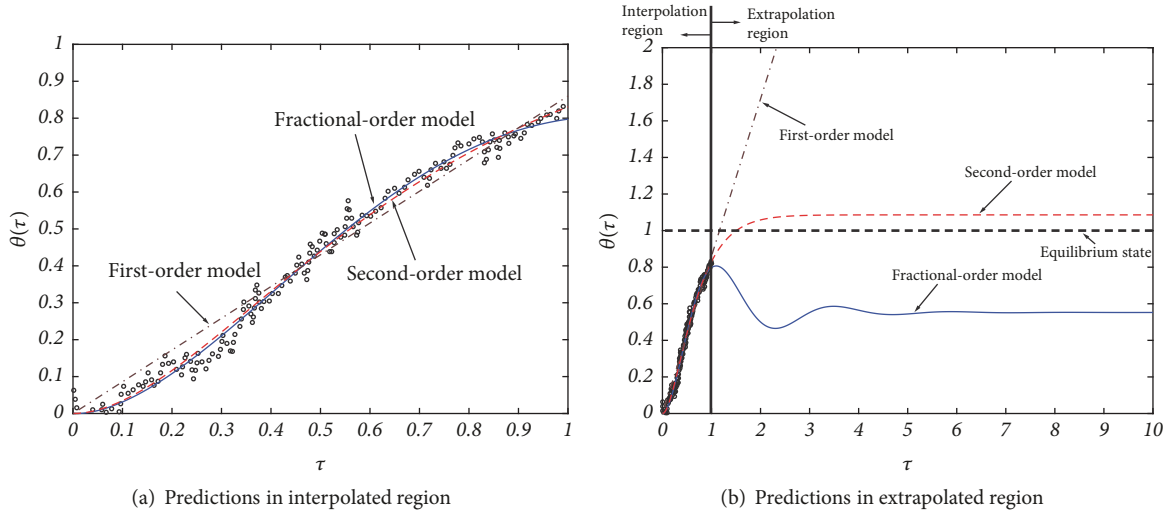
(b) Predictions in extrapolated region

FIGURE 5: Comparison in predictions from fractional- and integer-order fitted models.

fractional model with a value of $S_\theta = 6.647 \times 10^{-4}$, which is an improvement of 4.5% with respect to that of the model based on four parameters.

4.3. Reliability of the Model. The use of fractional-order approximation models stems from the fact that as the complexity of a system increases, so does its required mathematical representation. Though this can be achieved starting from conservation equations, for purposes of control it is important that the plant model is compact, efficient, and sufficiently accurate. For instance, a model based on the Navier-Stokes equations may be more accurate than an approximate model, but would be computationally intensive for control (for design and prediction, on the other hand, the mathematical model needs to be accurate). An approximate model, however, may also serve the purpose of bringing the output close to the desired state from where some other form of nonmodel control (e.g., PID) can take over. From this perspective, the fractional-order model given in (11) and (16) can be regarded simply as an approximation to the governing equations (PDEs), and certainly it is not a model based on first principles (i.e., derived from the laws of physics for a specific problem), but is developed based on a curve-fitting process from a set of experimental data in a specific domain. Thus, it follows that the resulting mathematical model can only be expected to perform well in the domain of the data from which it was derived (i.e., interpolation). In other words, the model may not work – and it does *not* have to work – beyond the domain in which the data apply (i.e., within the cloud of training data). Making predictions outside the domain of the data from which the model was derived would correspond to extrapolation, and therefore unreliable.

This data-driven model interpolation/extrapolation issue is particularly problematic for the case of complex systems, an example of which is heat exchangers, and the phenomena associated with them. In these thermal systems, complexity arises from geometrical configurations, the large number of parameters involved in their operation, and the nonlinear

nature of the system. In the latter case, for example, there is nonlinearity due to variation of properties (e.g., density, viscosity, and thermal conductivity), with temperature. Nonlinearity in the phenomena then generates the possibility of bifurcations, including instability and transition to turbulence. Finally, the conservation equations themselves, which provide the most accurate description of the system, are nonlinear (e.g., in the advective terms). It is apparent that nonlinearities associated with the system may be a main reason for constraining predictions from data-driven models to within the interpolation region only.

The issue of interpolation vs. extrapolation is prevalent in models derived from experimental data. For instance, techniques such as artificial neural networks and correlation equations, among others, are unreliable for extrapolation; yet, they are extremely useful for predictions *within* the region of training data of the system behavior at operating points different from those used to derive the model. This is illustrated in Figure 5 in the context of the current investigation, which shows the results from the fractional-order model given in (16) and an ordinary second-order linear oscillator given by

$$c_1 \frac{d^2\theta(\tau)}{d\tau^2} + c_3 \frac{d\theta(\tau)}{d\tau} + c_2 \theta(\tau) = u(\tau), \qquad (18)$$

with $y \equiv \theta$, zero initial conditions, and fitted constants c_1, c_2, and c_3 obtained from the same data. The figure shows the evolution of $\theta(\tau)$ for the ranges $\tau \in [0, 1]$ and $\tau \in [1, 10]$. For completeness, the results from a first-order model are also included. From Figure 5(a), the results show that, in the range $\tau \in [0, 1]$, both models predict the behavior of the system very well, with the fractional-order model being more accurate ($S_\theta = 6.94 \times 10^{-4}$ and $S_\theta = 7.72 \times 10^{-4}$, respectively), and both show (see Figure 5(b)) some discrepancy with respect to the expected behavior in the range $\tau \in [1, 10]$, with the second-order model being qualitatively more accurate than the fractional-order. However, in this range the actual values
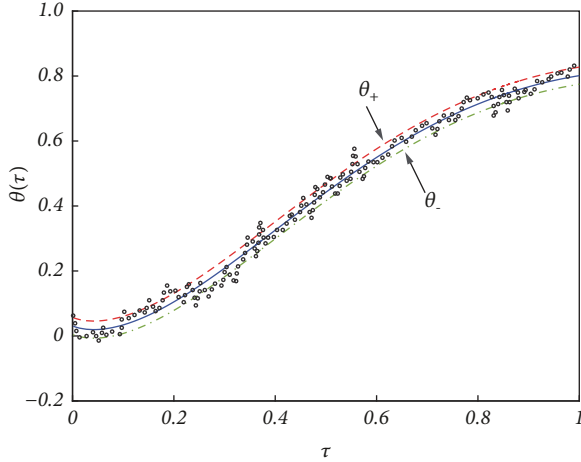
FIGURE 6: Range of applicability of five-parameter set $\mathbf{C}$ $=$ $(q, c_1, c_2, P_1 = \theta(0), P_2 = \theta'(0))$ model. $\theta_+ = \theta + \epsilon_{rms}$; $\theta_- = \theta - \epsilon_{rms}$.

of the expected behavior from both models are incorrect, indicating a lack of reliability.

The issue of reliability of mathematical models is an active research topic [38], and several studies have attempted to establish the region of reliability by defining it either as a hyperbox or by using the convex hull of the data. Others have concluded that the number and distribution of the experimental data are important factors in the reliability of empirical models [39, 40]. In fact, in the context of modeling with artificial neural networks, Pacheco-Vega et al. [41] discovered that even inside the cloud of data – and its corresponding convex hull – extrapolation could exist if the number and distribution of data points in a high-dimensional parameter space were limited in number and location, and proposed a methodology to establish the upper limits in the prediction error from such models.

4.4. Range of Applicability. In practice, experimental uncertainty may be present due to nonideal sensor measurement, thus it may be necessary to establish the applicability of the resulting model for the system under analysis. In the present case, we use the experimental data, along with a definition based on the root-mean-square (RMS) error, to establish the range of applicability for the five-parameter fractional-order model, i.e., (16), with fitted $\theta(0)$ and $\theta'(0)$.

The first step is to define the RMS error as

$$\epsilon_{rms} = \left[\frac{1}{N} \sum_{i=1}^{N} \left(\theta_i^p - \theta_i^e \right)^2 \right]^{1/2}. \tag{19}$$

This error provides the baseline value for the range of applicability from the original predictions. The next step is to shift the data up and down by a value ϵ_{rms}, as

$$\{\theta_+, \theta_-\} = \theta \pm \epsilon_{rms}. \tag{20}$$

The global-regression-based SI is then applied to the shifted data and the optimal parameters obtained. The results are given in Table 2 and Figure 6. Table 2 presents a quantitative

account of the results showing the range of applicability of the fractional differential equation model, where the order of the equation remains essentially unaltered, while the other θ_+- and θ_--based shifted parameters provide the values corresponding to the upper and lower bounds. Figure 6 supplies a graphical account of the same results, where it is clear that the model is able to accurately predict the behavior of the system.

5. Multiroom Building Data

The second test deals with a more complex multiroom building system. A subscaled two-floor building facility, designed specifically to be a scaled model of an actual building for energy-related studies, is located in the thermofluids laboratory at the California State University, Los Angeles, and is used to conduct experiments for thermal analysis and control [42]. A schematic of the experimental facility, with overall dimensions of 1.2 m $\times$ 0.92 m $\times$ 1.1 m, and its photographic depiction are shown in Figure 7. The test bed has a two-floor configuration with four rooms in each floor. Its structure is made of wood with interior walls covered with drywall and insulation (additional details are in [42]). Average temperatures of air in the rooms are measured by type-K thermocouples, while incandescent light bulbs serve as internal heat sources. Supply and return vents are installed in each room, and an external cooling unit is used to provide cold air through a set of ducts, each connected to the corresponding supply vent. Flow rates of air delivered into each room can be modified by a set of dampers (valves) through Arduino microcontrollers. Time-dependent information of the room temperatures, T, is collected in two DAQ boards and stored in a PC for further analysis. LabVIEW serves to interface the controller and the experimental system. The facility has been recently studied by Baltazar et al. [43] in the context of thermal control with fuzzy logic.

The average air temperature measurements for the eight rooms of the building are illustrated in Figure 8 which shows that each room is initially heated to a temperature above 27°C and then cooled down for 30 min [43]. From the figure it can be seen that all temperature curves depict three features: (1) the cooling rate in each room is different due to uneven delivery of airflow by the dampers; (2) there is a nearly exponential decay in the average temperatures, which is expected due to the convection process that takes place in each room; and (3) the decay in the temperatures is altered by two peaks, at $t = 17$ min and $t = 25$ min, resulting from the influence that the laboratory temperature has on the operation of the cooling unit.

For the analysis that follows, room 1 is selected because of its smooth transition from a maximum temperature, T_{max}, to a temperature considered as minimum, T_{min}, just before the peak occurs at t_{max}. As before, it is useful to normalize its mean temperature $T(t)$ and the time variable t, as

$$\theta(t) = \frac{T(t) - T_{min}}{T_{max} - T_{min}}; \quad \tau = \frac{t}{t_{max}}, \tag{21}$$

where θ is the dimensionless average temperature for air, τ the dimensionless time, $T_{max} = 28°C$, $T_{min} = 18°C$, and
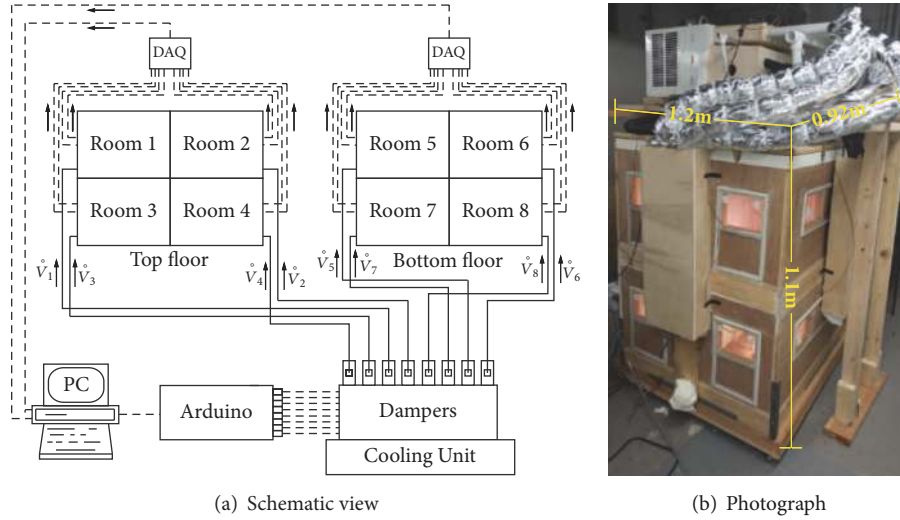
(a) Schematic view

(b) Photograph

FIGURE 7: Subscaled building test facility.
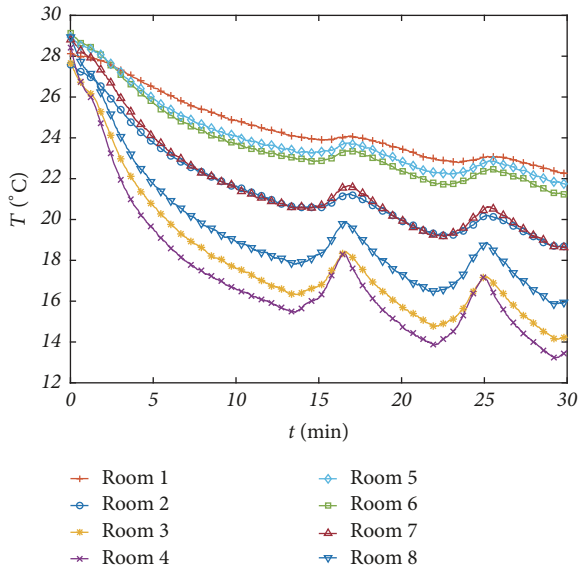
FIGURE 8: Time evolution of average room temperatures in multiroom building device.

○ Building test-bed data

FIGURE 9: Prediction of time evolution of average room temperature for room 1 from fractional-order models.

$t_{max} = 17$ min. With the aforementioned definitions, the linear fractional-order model is again defined as

$$c_1 \frac{d^q \theta (\tau)}{d\tau^q} + c_2 \theta (\tau) = u (\tau), \quad (22)$$

where $u(\tau)$ results from the sudden change in the delivery of cooling air flow from zero to a maximum.

The FOSI methodology is now applied to the experimental temperature measurements of room 1 of the test facility. Again, the variance of the error is $S_\theta = [\sum_{i=1}^{N}(\theta_i^p - \theta_i^e)^2]/N$, the parameter set is $\mathbf{C} = (q, c_1, c_2, P_1 = \theta(0), P_2 = \theta'(0))$, and the parameter search is constrained to the following ranges: $q \in [0, 2]$, $\{c_1, c_2\} \in [-10, 10]$, $\theta(0) \in [-10, 10]$, and $\theta'(0) \in [-10, 10]$. Using the same conditions, LOA is also used for

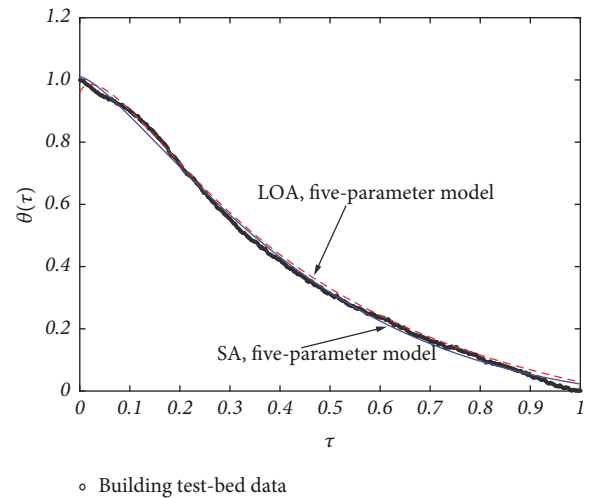purposes of comparison. The results from the two methods are shown in Figure 9 and Table 3, where it is clear that, once again, multiplicity of solutions for the parameter set $\mathbf{C}$, and $S_\theta(\mathbf{C})$, occurs. From the figure it can be observed that the fractional-order model obtained by the FOSI, SA technique, accurately predicts the dynamic behavior of the temperature dynamics in room 1 for the entire time range. It is particularly remarkable that the conditions of θ and θ' at $\tau = 0$ are very close to those of the data. On the other hand, the results from the LOA-based model are close to the measurements in the mid-section, but deviate significantly at the extremes, particularly near the initial times.

These results are confirmed quantitatively in Table 3, where it is noticed that the fractional-order model obtained via global regression outperforms the corresponding LOA model by close to 40% improvement in the accuracy of the predictions. Moreover, the values of the parameters

TABLE 3: Model parameters for the relaxation process in room 1 of a building test facility.

Model	q	c_1	c_2	$P_1 = \theta(0)$	$P_2 = \theta'(0)$	$S_\theta \times 10^4$
SA	1.2319	3.4428	10	1.0223	-0.1043	2.04
LOA	1.0266	-0.0213	-0.1052	0.9577	47.5124	2.86

obtained from global regression seem to be consistent with the experimental data, particularly those of the rate of change in temperature θ', at times close to zero, whereas those computed by the LOA technique can be associated with physically unfeasible conditions, as mentioned in the previous section.

Finally, it is important to note that, though commonly done with integer-order calculus, a physical interpretation of the fractional derivative in the modeling of the two thermal systems analyzed here is not necessary since the corresponding fractional-order model – in each case – is merely a stand-in for the true mathematical model. Some efforts have been made in the physical interpretation of fractional-order derivatives (see [44, 45], for example), but at the moment they do not have the acceptance that terms such as velocity and acceleration have in mechanics, for instance. The issue of the physical interpretation of fractional-order models would become more important if initial conditions were being assigned based on the initial state of the plant.

6. Concluding Remarks

Complex systems, of which heat exchangers and multiroom buildings are examples, can be found in widespread applications. For their performance control it is necessary to obtain an accurate description of their dynamic behavior. In this regard, fractional-order differential equations, derived via SI, may provide compact and efficient models of complex systems. In this work, a fractional-order-based system SI procedure grounded on global regression has been proposed to build accurate models from data. The SI methodology seeks the optimum values of a parameter set that includes the fractional order of the differential equation, its parametric constants, and, when necessary, the initial conditions. This last case arises when accurate knowledge of the initial conditions, whether the value of the function or its rate of change, is not possible, and such conditions have to be included as part of the search. It is to be noted, however, that there may be cases when some values of these conditions may not be physically feasible.

The application of the SI methodology to experimental measurements from a shell-and-tube heat exchanger and a multiroom building has confirmed that the approach is accurate and robust. The fractional-based model obtained via global regression provides better approximations to the data than those obtained by SI with local optimization algorithms. The results show that not only the apparent multiplicity in the parameter set that includes the order of the proposed model equation along with its constants and the initial conditions, as provided by the results from the global regression analysis, is due to the fact that the initial condition(s) is(are) included in the search, rather than in the model itself, but also the proposed fractional-order differential equation model is reliable within the interpolation region, but cannot be used with confidence for predictions outside this region. The SI methodology proposed here is robust and can be used to derive accurate and compact models from experimental data. In addition, given a functional form of a fractional-order differential equation model, as new data become available the SI technique can be used to expand the region of reliability (interpolation) of the resulting model. The methodology described here can be extended to model other complex physical systems.

Nomenclature

J^α: Fractional integral operator of order α
c_1, c_2:   Coefficient for the linear fractional differential equation
D_{RL}^α: Riemann-Liouville fractional derivative of order α
D_C^α: Caputo fractional derivative of order α
$E_{i,j}$:   Two-parameter Mittag-Leffler function
m: m-th integer order
$\dot{m}$:   Mass flow rate
P_k: k-th initial condition
q: Fractional order
S_y, S_θ: Variance of the error
N: Number of experimental data points
$\mathbf{C}$:   Vector of search parameters
T: Fluid bulk temperature [K]
t: Time [s]
$u(t)$:   Input variable
$y(t)$:   Output variable

Greek Symbols

ϵ: rms error
$\Gamma(\xi)$:   Gamma function
θ: Dimensionless temperature
ξ: Independent variable
τ: Dimensionless time

Subscripts and Superscripts

c: Cold fluid
e: Experimental value
h: Hot fluid
in: Inlet
out: Outlet
p: Predicted value

Abbreviations

DAQ: Data acquisition system
FDE: Fractional-order differential equation
FOSI Fractional-order system identification
LOA: Local optimization algorithm
ODE: Ordinary differential equation
SA: Simulated annealing algorithm
SI: System identification
PDE: Partial differential equation.

Data Availability

The data used in this study can be made available, after publication, via a hyperlink to the corresponding author's personal website.

Conflicts of Interest

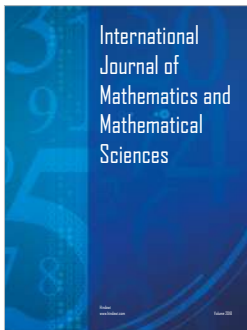The authors declare that they have no conflicts of interest.

Acknowledgments

References

[1] Z. S. Hou and Z. Wang, "From model-based control to data-driven control: survey, classification and perspective," *Information Sciences*, vol. 235, pp. 3–35, 2013.

[2] R. C. Dorf and R. H. Bishop, *Modern Control Systems*, Pearson, Upper Saddle River, 13th edition, 2016.

[3] A. Pacheco-Vega, C. Ruiz-Mercado, K. Peters, and L. E. Vilchiz, "On-line fuzzy-logic-based temperature control of a concentric-tube heat exchanger facility," *Heat Transfer Engineering*, vol. 30, no. 14, pp. 1208–1215, 2009.

[4] A. Pacheco-Vega, G. Diaz, M. Sen, and K. T. Yang, *Applications of artificial neural networks and genetic methods in thermal engineering*, R. P. Chhabra, Ed., chapter 4.27, CRC Handbook of Thermal Engineering, 2nd edition, 2017.

[5] G. Díaz, M. Sen, K. T. Yang, and R. L. McClain, "Adaptive neurocontrol of heat exchangers," *Journal of Heat Transfer*, vol. 123, no. 3, pp. 556–562, 2001.

[6] R. L. Bagley and R. A. Calico, "Fractional order state equations for the control of viscoelastically damped structures," *Journal of Guidance, Control, and Dynamics*, vol. 14, no. 2, pp. 304–311, 1991.

[7] C. A. Monje, Y. Chen, B. M. Vinagre, D. Xue, and V. Feliu, *Fractional-Order Systems and Controls*, Advances in Industrial Control, Springer, London, UK, 2010.

[8] V. E. Tarasov, *Fractional Dynamics: Applications of Fractional Calculus to Dynamics of Particles, Fields and Media*, Springer, Berlin, Germany, 2010.

[9] S. Das, *Functional Fractional Calculus*, Springer, New Delhi, India, 2011.

[10] J. T. Machado, V. Kiryakova, and F. Mainardi, "Recent history of fractional calculus," *Communications in Nonlinear Science and Numerical Simulation*, vol. 16, no. 3, pp. 1140–1153, 2011.

[11] E. C. de Oliveira and J. A. Tenreiro Machado, "A review of definitions for fractional derivatives and integral," *Mathematical Problems in Engineering*, vol. 2014, Article ID 238459, 6 pages, 2014.

[12] M. D. Ortigueira and J. A. Tenreiro Machado, "What is a fractional derivative?" *Journal of Computational Physics*, vol. 293, pp. 4–13, 2015.

[13] S. Kirkpatrick, C. D. Gelatt, and M. P. Vecchi, "Optimization by simulated annealing," *Science*, vol. 220, no. 4598, pp. 671–680, 1983.

[14] I.-K. Jeong and J.-J. Lee, "Adaptive simulated annealing genetic algorithm for system identification," *Engineering Applications of Artificial Intelligence*, vol. 9, no. 5, pp. 523–532, 1996.

[15] K. B. Oldham and J. Spanier, *The Fractional Calculus: Theory and Applications of Differentiation and Integration to Arbitrary Order*, Academic Press, New York, NY, USA, 1974.

[16] S. G. Samko, A. A. Kilbas, and O. I. Marichev, *Fractional Integrals and Derivatives: Theory and Applications*, Gordon and Breach Science Publishers, 1993.

[17] I. Podlubny, *Fractional Differential Equations*, vol. 198 of *Mathematics in Science and Engineering*, Academic Press, San Diego, Calif, USA, 1999.

[18] L. Vlahos, H. Isliker, Y. Kominis, and K. Hizanidis, "Normal and anomalous diffusion: A tutorial," 2008, https://arxiv.org/abs/0805.0419.

[19] B. Goodwine, "Modeling a multi-robot system with fractional-order differential equations," in *Proceedings of the 2014 IEEE International Conference on Robotics and Automation (ICRA)*, pp. 1763–1768, Hong Kong, China, May 2014.

[20] M. Sen, J. P. Hollkamp, F. Semperlotti, and B. Goodwine, "Implicit and fractional-derivative operators in infinite networks of integer-order components," *Chaos, Solitons and Fractals*, vol. 114, pp. 186–192, 2018.

[21] K. A. Lazopoulos, D. Karaoulanis, and A. K. Lazopoulos, "On fractional modelling of viscoelastic mechanical systems," *Mechanics Research Communications*, vol. 78, pp. 1–5, 2016.

[22] Y. Aoki, M. Sen, and S. Paolucci, "Approximation of transient temperatures in complex geometries using fractional derivatives," *Heat and Mass Transfer*, vol. 44, no. 7, pp. 771–777, 2008.

[23] S. M. Pineda, G. Diaz, and C. F. Coimbra, "Approximation of transient 1D conduction in a finite domain using parametric fractional derivatives," *Journal of Heat Transfer*, vol. 133, no. 7, p. 071301, 2011.

[24] J.-D. Gabano and T. Poinot, "Fractional modelling and identification of thermal systems," *Signal Processing*, vol. 91, no. 3, pp. 531–541, 2011.

[25] R. Caponetto, F. Sapuppo, V. Tomasello, G. Maione, and P. Lino, "Fractional-order identification and control of heating processes with non-continuous materials," *Entropy*, vol. 18, no. 11, article 398, 2016.

[26] M. Caputo, "Linear models of dissipation whose Q is almost frequency independent-II," *The Geophysical Journal of the Royal Astronomical Society*, vol. 13, no. 5, pp. 529–539, 1967.

[27] G. N. Vanderplaats, *Numerical Optimization Techniques for Engineering Design: With Applications*, National Science Review, Mineola, New York, NY, USA, 1984.

[28] D. E. Goldberg, *Genetic Algorithms in Search, Optimization, and Machine Learning*, Addison-Wesley, 1989.

[29] E. Aarts and J. Korst, *Simulated Annealing and Boltzmann Machines*, Wiley-Interscience Series in Discrete Mathematics and Optimization, John Wiley & Sons, Chichester, UK, 1989.

[30] F. Archetti and F. Schoen, "A survey on the global optimization problem: General theory and computational approaches," *Annals of Operations Research*, vol. 1, no. 2, pp. 87–110, 1984.

[31] A. Gotmare, S. S. Bhattacharjee, R. Patidar, and N. V. George, "Swarm and evolutionary computing algorithms for system identification and filter design: A comprehensive review," *Swarm and Evolutionary Computation*, vol. 32, pp. 68–84, 2017.

[32] N. Metropolis, A. W. Rosenbluth, M. N. Rosenbluth, A. H. Teller, and E. Teller, "Equation of state calculations by fast computing machines," *The Journal of Chemical Physics*, vol. 21, no. 6, pp. 1087–1092, 1953.

[33] A. Corana, M. Marchesi, C. Martini, and S. Ridella, "Minimizing multimodal functions of continuous variables with the 'simulated annealing' algorithm," *ACM Transactions on Mathematical Software*, vol. 13, no. 3, pp. 262–280, 1987.

[34] A. Pacheco-Vega, M. Sen, and K. T. Yang, "Simultaneous determination of in- and over-tube heat transfer correlations in heat exchangers by global regression," *International Journal of Heat and Mass Transfer*, vol. 46, no. 6, pp. 1029–1040, 2003.

[35] E. R. Hansen, *Global Optimization using Interval Analysis*, vol. 165, Marcel Dekkar, New York, NY, USA, 1992.

[36] J. Mayes, *Reduction and Approximation in Large and Infinite Potential-Driven Flow Networks [Ph.D. thesis]*, University of Notre Dame, Notre Dame, Indiana, 2012.

[37] K. M. Li, M. Sen, and A. Pacheco-Vega, "Fractional-Order-Based System Identification for Heat Exchangers," in *Proceedings of the The 3rd World Congress on Momentum, Heat and Mass Transfer*, Budapest, Hungary, April 2018.

[38] J. Fan, F. Han, and H. Liu, "Challenges of big data analysis," *National Science Review*, vol. 1, no. 2, pp. 293–314, 2014.

[39] P. Courrieu, "Three algorithms for estimating the domain of validity of feedforward neural networks," *Neural Networks*, vol. 7, no. 1, pp. 169–174, 1994.

[40] P. Niyogi and F. Girosi, "Generalization bounds for function approximation from scattered noisy data," *Advances in Computational Mathematics*, vol. 10, no. 1, pp. 51–80, 1999.

[41] A. Pacheco-Vega, M. Sen, K. T. Yang, and R. L. McClain, "Neural network analysis of fin-tube refrigerating heat exchanger with limited experimental data," *International Journal of Heat and Mass Transfer*, vol. 44, no. 4, pp. 763–770, 2001.

[42] A. Baghdasarian, O. Ramos, J. Ruvalcaba et al., "Design and instrumentation of an experimental test-bed for research in energy efficiency in buildings," in *Proceedings of the ASME 2015 International Mechanical Engineering Congress and Exposition, IMECE 2015*, Houston, USA, November 2015.

[43] J. Baltazar, A. Yarian, and A. Pacheco-Vega, "Development of P-PD- and PID-fuzzy SISO controllers of a sub-scaled multi-room building test-bed," in *Proceedings of the 3rd Thermal and Fluids Engineering Conference (TFEC)*, Tampa, USA, March, 2018.

[44] J. F. Gómez-Aguilar, R. Razo-Hernández, and D. Granados-Lieberman, "A physical interpretation of fractional calculus in observables terms: analysis of the fractional time constant and the transitory response," *Revista Mexicana de Física*, vol. 60, no. 1, pp. 32–38, 2014.

[45] V. E. Tarasov, "Interpretation of fractional derivatives as reconstruction from sequence of integer derivatives," *Fundamenta Informaticae*, vol. 151, no. 1-4, pp. 431–442, 2017.